



Bound states in the continuum and Fano resonances in the Dirac cone spectrum

EVGENY N. BULGAKOV^{1,2} AND DMITRII N. MAKSIMOV^{1,2,3,*}

¹Reshetnev Siberian State University of Science and Technology, 660037, Krasnoyarsk, Russia

²Kirensky Institute of Physics, Federal Research Center KSC SB RAS, 660036, Krasnoyarsk, Russia

³Siberian Federal University, 660041, Krasnoyarsk, Russia

*Corresponding author: mdn@tnp.krasn.ru

Received 8 May 2019; revised 21 June 2019; accepted 27 June 2019; posted 2 July 2019 (Doc. ID 367081); published 26 July 2019

We consider light scattering by two-dimensional arrays of high-index dielectric spheres arranged into a triangular lattice. It is demonstrated that in the case of a triple degeneracy of resonant leaky modes in the gamma point, the scattering spectra exhibit a complicated picture of Fano resonances with extremely narrow linewidth. The Fano features are explained through coupled-mode theory for a Dirac cone spectrum as a signature of optical bound states in the continuum (BIC). It is found that the standing wave in-gamma BIC induces a ring of off-gamma BICs due to different scaling laws for real and imaginary parts of the resonant eigenfrequencies in the Dirac cone spectrum. A quantitative theory of the spectra is proposed. © 2019 Optical Society of America

<https://doi.org/10.1364/JOSAB.36.002221>

1. INTRODUCTION

Photonic band engineering plays an important role in modern science and technology [1,2]. Among numerous implementations, attention has been paid to photonic crystalline designs supporting the Dirac cone spectrum about the Γ point, which paves a way to all-dielectric zero-refractive-index materials [3,4]. Recently, zero-index all-dielectric metamaterials have been proposed [5], relying on the effect of optical bound states in the continuum (BICs), which are lossless localized solutions coexisting with the continuous spectrum of the scattering states [6,7]. The emergence of BICs is remarkable due to their effect on the scattering of electromagnetic waves. The BICs are known to induce sharp Fano [8–12] resonances in the scattering spectra due to interference between two optical pathways: the resonant pathway via the subradiant mode associated with the BIC, and the direct pathway due to nonresonant scattering [12–16]. In principle, in the spectral vicinity of a BIC, the Q factor of the resonances can be tuned to arbitrary high value once the material losses are neglected [17,18]. In this paper, we examine the effect of the radiation losses on the spectrum of the leaky bands and Fano resonances about the Dirac point in a dielectric structure extended in two dimensions.

2. SPECTRUM OF LEAKY MODES AND FANO RESONANCES

We consider a periodic two-dimensional (2D) array of high-contrast ($\epsilon = 15$) dielectric spheres of radius R arranged into a triangular lattice in the $x0y$ plane with period a , as shown in Fig. 1. Further on, the frequency will be expressed in terms of

the vacuum wave vector k_0 . To recover the optical properties of the system, we employ the Korringa–Kohn–Rostoker (KKR) method, which was adapted to scattering of electromagnetic (EM) waves by 2D arrays of dielectric spheres by Ohtaka [19,20]. The method was later generalized for finding the band structure [21]. Here the KKR method has been directly applied according to [19–21] for both the band structure and scattering spectra. The primary advantage of the method is a straightforward implementation of the Mie solutions for individual spheres, which results in a set of equations for multipolar expansion coefficients. The numerical data presented in the paper are obtained with four multipoles. The convergence has been checked by increasing the number of multipoles with no significant effect.

The triangular lattice complies with the C_{6v} point symmetry group [22], which has four one-dimensional (A_1, A_2, B_1, B_2) and two 2D representations (E_1, E_2). According to Sakoda [23], a Dirac cone can be engineered through a triple degeneracy between two modes, p_x and p_y , of irreducible representation E_1 , and one mode, s , of irreducible representation A_1 in the Γ point. p_x and p_y have the same frequency Ω_1 in the Γ point, since they are of the same irreducible representation. The s mode, though, generally has a different frequency Ω_2 . The degeneracy $\Omega_1 = \Omega_2$ is accidental in nature and can be obtained by tuning the radius of the spheres. In the case of $\epsilon = 15$, the degeneracy is found at $R = 0.4705a$. Once the degeneracy is achieved, the spectrum in the vicinity of the Γ point consists of an isotropic Dirac cone and a quadratic dispersion surface [23].

The spectrum of the leaky modes against the x component of the wave vector, k_x , is shown in Fig. 2. One can see in Fig. 2

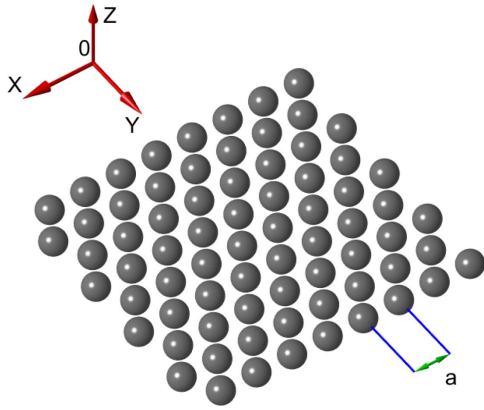


Fig. 1. Triangular lattice of dielectric spheres.

that the real parts of the eigenfrequencies demonstrate a behavior very close to that predicted in Ref. [23], with two bands forming a Dirac cone while the third, weakly dispersive band is parabolic. The Dirac spectrum in the x direction is formed by hybridization between s and p_x modes, which both have their electric fields antisymmetric with respect to $y \rightarrow -y$. Notice that the radiation losses result in an anomaly in the spectrum, with the dispersion deviating from a Dirac cone at small values of k_x , as can be seen from the insets. That anomaly associated with an exceptional point has been considered in detail by Zhen and co-authors [24]. We mention in passing that the electric vector of p_y mode is symmetric with respect to $y \rightarrow -y$. At the same time, both s and p_y are antisymmetric with respect to $x \rightarrow -x$, while p_x is symmetric. For a detailed analysis of mode symmetries on the triangular lattice, we address the reader to [25].

More interesting, though, is the behavior of the imaginary parts of the eigenfrequency, which correspond to the widths of the resonances. In the Γ point, the low-frequency band obtains zero imaginary parts, which indicates the emergence of symmetry-protected BIC standing waves decoupled from outgoing

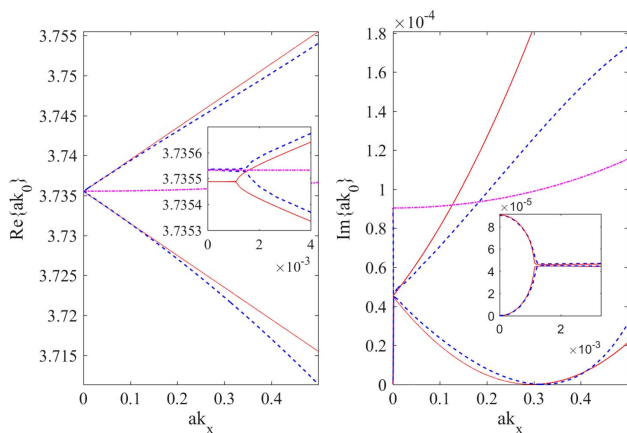


Fig. 2. Spectrum of leaky bands in the vicinity of the Γ point. The real part of the eigenfrequency, left panel; the imaginary part, right panel. The insets resolve the spectra to $ak_x \approx 10^{-3}$. The dashed blue lines show the spectrum of the hybridized modes; dashed-dotted magenta lines, the p_y mode. The red lines are eigenvalues of the matrix Eq. (3).

waves by symmetry [5]. The other two modes, p_x and p_y , are leaky in the Γ point. With the slightest offset in the k space, the imaginary parts undergo dramatic changes due to hybridization between the s and p_x modes. That results in almost equal imaginary parts at $ak_x \approx 10^{-3}$. Then, the imaginary part of the high-frequency band gradually increases with k_x , while the imaginary part of the low-frequency band drops to zero at $ak_x \approx 0.317$, where we find the second BIC. Since the BICs of that type have a nonzero wave vector along the axis of periodicity of the structure, they are termed Bloch BICs [13].

Next, we propose a simple phenomenological approach explaining the structure of the spectrum in Fig. 2. According to [23], the spectrum of hybridized modes of E_1 and A_1 representations is found as the eigenvalues of the “Hamiltonian” matrix

$$C_0 = \begin{pmatrix} 0 & 0 & bk_x \\ 0 & 0 & bk_y \\ b^*k_x & b^*k_y & 0 \end{pmatrix}, \quad (1)$$

where b is a constant that can be evaluated by solving Maxwell’s equations numerically [23]. Assume that the propagation direction of the incident wave is orthogonal to the y axis, i.e., $k_y = 0$. Then Eq. (1) is reduced to a 2×2 matrix,

$$H_0 = \begin{pmatrix} 0 & bk_x \\ b^*k_x & 0 \end{pmatrix}. \quad (2)$$

The radiation losses can be incorporated into Eq. (2) by applying coupled-mode theory [26] for the hybridized resonances in the following manner:

$$H = H_0 + \frac{i}{2} W^\dagger W, \quad (3)$$

where $W^\dagger = (\sqrt{\gamma_p}, \sqrt{\gamma_s})$, with γ_s and γ_p being the decay rates of the hybridizing s and p_x modes into the TE wave radiation channel with the TE outgoing (incoming) wave being defined as that whose electric vector is perpendicular to the plane of incidence. Notice that for $k_y = 0$, the hybridized modes are decoupled from the TM wave by symmetry. Having in mind the definition of Eq. (3), the quantity γ_p can be found from Fig. 2 as one-half of the imaginary part of the resonant eigenfrequency of the p_x mode in the Γ point. Here we found $a\gamma_p = 9.040 \cdot 10^{-4}$. On the other hand, γ_s in the vicinity of the Γ point must be a dispersive quantity to reflect the singular nature of the symmetry-protected BIC [14]. The leading term in the k_x expansion of γ_s is quadratic, since $k_x = 0$ is the absolute minimum of the linewidth corresponding to the symmetry-protected BICs. The dispersion of γ_s can be accessed by slightly detuning the radius R to lift the degeneracy so the individual features of the s mode can be resolved. By running simulations with $R = 0.4514$, one finds $a\gamma_s = 1.028 \cdot 10^{-3} \cdot k_x^2$. Finally, the parameter b can be found via the perturbative approach in Ref. [23], or simply extracted from Fig. 2 as the real parts’ repulsion rate away from the feature at $ak_x \approx 10^{-3}$. Here we found $b = 0.04$. In Fig. 2, we demonstrate the spectrum of the matrix Eq. (3), which is found to be in quantitative agreement with numerical data. One can see that the model predicts the emergence of the satellite Bloch BIC as well as the anomalous spectral feature in the immediate vicinity of the Γ point.

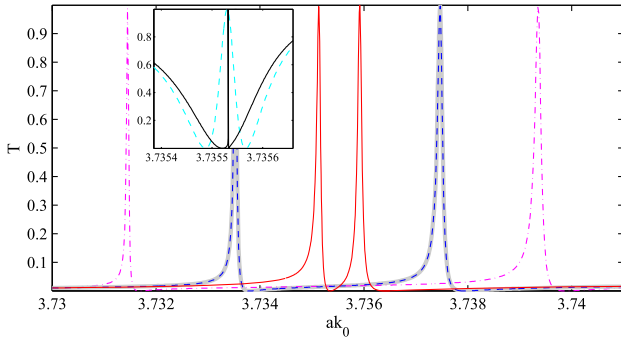


Fig. 3. Transmittance spectrum of the TE wave, $k_y = 0$. Red line, $ak_x = 0.01$; blue dashed line, $ak_x = 0.05$; dashed-dotted magenta line, $ak_x = 0.1$. The inset shows the resonant feature in the vicinity of the exceptional point; teal dashed line, $ak_x = 10^{-3}$; solid black line, $ak_x = 8 \cdot 10^{-5}$. The thick gray line shows the case of the TE wave with $ak_x = 0$, $ak_y = 0.05$.

Now, let us discuss the effect of the spectra on the scattering. It is known that the presence of high- Q leaky modes results in narrow Fano features that collapse as the spectral parameters are tuned to a BIC [12–14,16]. In our situation, away from the exceptional point, the TE wave scattering should reveal two isolated Fano resonances whose positions are given by the real parts of the Dirac cone eigenfrequencies, while the width is controlled by the imaginary part of the spectrum. That statement is in full agreement with the numerical data shown in Fig. 3. In the vicinity of the exceptional point, the Fano resonances merge into a single feature, which can only be resolved on a zoomed scale in k_0 , as shown in the inset in Fig. 3. Finally, we mention in passing that TM waves are only coupled to the single parabolic band, resulting in a single, almost nondispersive Fano feature.

3. RING OF BICS

What is remarkable, according to Eq. (1), is that the Dirac cone is isotropic in the momentum space in the vicinity of the Γ point. Let us see whether the presence of the radiation losses breaks that symmetry. Let us specify the propagation direction specified by arbitrarily azimuthal angle ϕ such that $k_x = k_{\parallel} \cos(\phi)$ and $k_y = k_{\parallel} \sin(\phi)$ with $k_{\parallel} = \sqrt{k_x^2 + k_y^2}$. The Hamiltonian has to be written in the following form [26]:

$$C = C_0 + \frac{i}{2} W^\dagger W, \quad (4)$$

where W is a 2×3 matrix composed of the row matrices, $W = [W_{\text{TE}}, W_{\text{TM}}]$, which describe the coupling with TE and TM waves, correspondingly. Taking into account that $p_x \rightarrow p_y$ and $p_y \rightarrow -p_x$ under rotation by $\phi = \pi$, we can write

$$W_{\text{TE}} = \left[\sqrt{\gamma_p} \cos(\phi), \sqrt{\gamma_p} \sin(\phi), \sqrt{\gamma_s} \right], \quad (5)$$

$$W_{\text{TM}} = \left[-\sqrt{\gamma_p} \sin(\phi), \sqrt{\gamma_p} \cos(\phi), 0 \right]. \quad (6)$$

Next, one can easily check that after transforming the Hamiltonian $C' = R^\dagger C R$ with matrix R ,

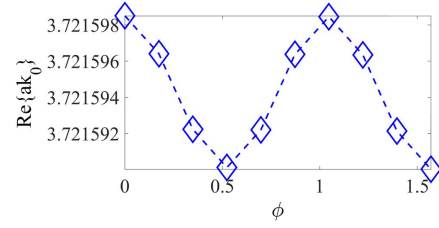


Fig. 4. Eigenfrequencies of the off- Γ BICs as the function of the azimuthal angle ϕ .

$$R = \begin{pmatrix} \cos(\phi) & -\sin(\phi) & 0 \\ \sin(\phi) & \cos(\phi) & 0 \\ 0 & 0 & 1 \end{pmatrix}, \quad (7)$$

one finds

$$C' = \begin{pmatrix} 0 & 0 & bk_{\parallel} \\ 0 & 0 & 0 \\ b^* k_{\parallel} & 0 & 0 \end{pmatrix} + \frac{i}{2} \begin{pmatrix} \gamma_p & 0 & \sqrt{\gamma_s \gamma_p} \\ 0 & \gamma_p & 0 \\ \sqrt{\gamma_s \gamma_p} & 0 & \gamma_s \end{pmatrix}, \quad (8)$$

which reduces to Eq. (3) in terms of coupling to the TE wave. Moreover, one can immediately see that the spectrum of complex eigenfrequencies is invariant under rotation. It means that our observation on the TE wave scattering applies for any orientation of the plane of incidence given by ϕ . This statement is illustrated in Fig. 3 for the incident wave with $k_x = 0$,

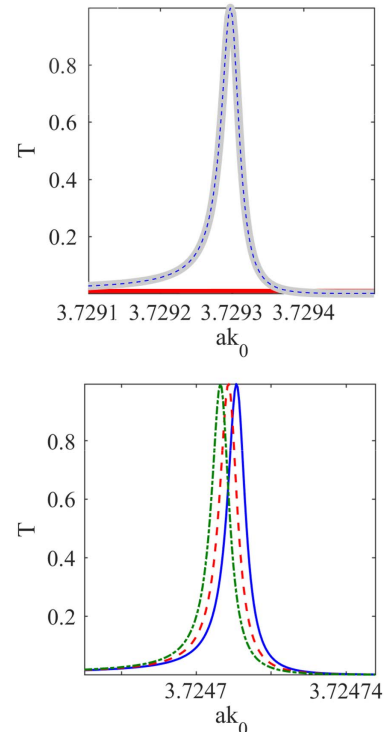


Fig. 5. Transmittance spectrum of TE waves in the vicinity of the ring of BICs. Upper panel, $ak_{\parallel} = 0.15$; thick gray line, $\phi = 0$; thin dashed blue line, $\phi = \pi/2$. Solid red line is the transmittance of TM waves. Lower panel, $ak_{\parallel} = 0.25$; solid blue line, $\phi = 0$; dashed red line, $\phi = \pi/4$; dashed-dotted green line, $\phi = \pi/2$.

$ak_y = 0.05$. Since the two-state model applies for any ϕ , the frequencies of the satellite Bloch BIC form a ring around the Γ point.

In Fig. 4, we show the eigenfrequencies of the off- Γ BICs as a function of the azimuthal angle ϕ . One can see from Fig. 4 that the BICs form an almost ideally circular ring, with the lattice anisotropy footprint emerging only in the seventh significant digit. Let us consider the transmittance spectrum in the immediate vicinity of the off- Γ BICs. Assume that the frequency of the incident wave is tuned to the lowest branch in Fig. 2. Then, if k_{\parallel} of the incident is matched to that of the leaky mode, the scattering spectrum of TE waves exhibits an extremely narrow Fano feature whose profile is almost independent of the azimuthal angle. This is illustrated in Fig. 5 (upper panel) for $ak_{\parallel} = 0.15$. In the same subplot, we also demonstrate that the resonant feature can be only observed with TE waves, while the transmittance of the TM waves remains independent of frequency on the scale of the Fano resonance. Finally, on the further approach to the ring of BICs, the lattice anisotropy emerges as a small shift of the resonance positions with respect to each other, as seen from Fig. 5 (lower panel).

4. CONCLUSION

In summary, here we went beyond the ring of exceptional points predicted in Ref. [24] by taking into account the dispersion of the hybridized mode linewidths. We have demonstrated that the presence of a Dirac cone in the Γ point results in the emergence of high- Q Fano resonances in the transmittance spectrum of TE waves near the normal incidence. The positions and widths of the resonances can be estimated from a simple coupled-mode approach, leading to a 2×2 matrix whose parameters are easily extracted from the dispersion of the hybridized leaky modes. It is shown that in the vicinity of the Γ point, the scattering spectra are insensitive to the orientation of the plane of incidence. Most remarkably, it is found that the presence of a Dirac cone together with an in- Γ symmetry-protected BIC induces a ring of Bloch BICs surrounding the Γ point and the k -space. The emergence of the BICs in the model is a result of destructive interference between two resonant modes with the condition for BICs [27] being fulfilled by tuning the wavenumber due to the difference in asymptotic behavior between Hermitian and non-Hermitian parts of the matrix in Eq. (3). Finally, we believe that a single parameter semianalytical model of the scattering spectra could be constructed by fitting the numerical spectrum to the coupled-mode solution [26]. That, however, falls out of the scope of the paper.

The presence of the BICs allows for fine-tuning the width of Fano resonances by changing the angle of incidence. Lately, we have seen a great deal of interest in the application of Fano resonances to sensing and switching [28–30]. More recently, topologically enabled ultrahigh Q resonances that are resistant to out-of-plane scattering were demonstrated due to the effect of a constellation of nine BICs about the Γ point [31]. The ring of BICs might potentially serve as an alternative to that approach, with the advantage of an isotropic dispersion of the Q factor. We believe that the proposed model may be a useful platform for engineering Fano resonances in all-dielectric setups [32]. The possibility of BICs eigenfrequencies forming a

ring in momentum space has been recently pointed out in a view of multipolar decompositions [33]. We speculate that a further detailed analysis of multipolar structure could shed light onto interference mechanisms leading to BICs.

Funding. Ministry of Higher Education and Science of the Russian Federation (State Contract N 3.1845.2017/4.6).

REFERENCES

1. Y. Ding and R. Magnusson, "Resonant leaky-mode spectral-band engineering and device applications," *Opt. Express* **12**, 5661–5674 (2004).
2. J. D. Joannopoulos, S. G. Johnson, J. N. Winn, and R. D. Meade, *Photonic Crystals: Molding the Flow of Light* (Princeton University, 2011).
3. X. Huang, Y. Lai, Z. H. Hang, H. Zheng, and C. T. Chan, "Dirac cones induced by accidental degeneracy in photonic crystals and zero-refractive-index materials," *Nat. Mater.* **10**, 582–586 (2011).
4. C. T. Chan, Z. H. Hang, and X. Huang, "Dirac dispersion in two-dimensional photonic crystals," *Adv. OptoElectron.* **2012**, 1–11 (2012).
5. M. Minkov, I. A. D. Williamson, M. Xiao, and S. Fan, "Zero-index bound states in the continuum," *Phys. Rev. Lett.* **121**, 263901 (2018).
6. C. W. Hsu, B. Zhen, A. D. Stone, J. D. Joannopoulos, and M. Soljačić, "Bound states in the continuum," *Nat. Rev. Mater.* **1**, 16048 (2016).
7. K. Koshelev, G. Favraud, A. Bogdanov, Y. Kivshar, and A. Fratallocchi, "Nonradiating photonics with resonant dielectric nanostructures," *Nanophotonics* **8**, 725–745 (2019).
8. J. Lee, B. Zhen, S.-L. Chua, W. Qiu, J. D. Joannopoulos, M. Soljačić, and O. Shapira, "Observation and differentiation of unique high- Q optical resonances near zero wave vector in macroscopic photonic crystal slabs," *Phys. Rev. Lett.* **109**, 067401 (2012).
9. C. S. Kim, A. M. Satanin, Y. S. Joe, and R. M. Cosby, "Resonant tunneling in a quantum waveguide: effect of a finite-size attractive impurity," *Phys. Rev. B* **60**, 10962 (1999).
10. S. P. Shipman and S. Venakides, "Resonant transmission near nonrobust periodic slab modes," *Phys. Rev. E* **71**, 026611 (2005).
11. A. F. Sadreev, E. N. Bulgakov, and I. Rotter, "Bound states in the continuum in open quantum billiards with a variable shape," *Phys. Rev. B* **73**, 235342 (2006).
12. C. Blanchard, J.-P. Hugonin, and C. Sauvan, "Fano resonances in photonic crystal slabs near optical bound states in the continuum," *Phys. Rev. B* **94**, 155303 (2016).
13. E. N. Bulgakov and A. F. Sadreev, "Light trapping above the light cone in a one-dimensional array of dielectric spheres," *Phys. Rev. A* **92**, 023816 (2015).
14. E. N. Bulgakov and D. N. Maksimov, "Optical response induced by bound states in the continuum in arrays of dielectric spheres," *J. Opt. Soc. Am. B* **35**, 2443–2452 (2018).
15. E. Bochkova, S. Han, A. de Lustrac, R. Singh, S. N. Burokur, and A. Lupu, "High- Q Fano resonances via direct excitation of an antisymmetric dark mode," *Opt. Lett.* **43**, 3818–3821 (2018).
16. A. A. Bogdanov, K. L. Koshelev, P. V. Kapitanova, M. V. Rybin, S. A. Gladyshev, Z. F. Sadrieva, K. B. Samusev, Y. S. Kivshar, and M. F. Limonov, "Bound states in the continuum and Fano resonances in the strong mode coupling regime," *Adv. Photon.* **1**, 016001 (2019).
17. L. Yuan and Y. Y. Lu, "Strong resonances on periodic arrays of cylinders and optical bistability with weak incident waves," *Phys. Rev. A* **95**, 023834 (2017).
18. E. Bulgakov and A. Sadreev, "Fibers based on propagating bound states in the continuum," *Phys. Rev. B* **98**, 085301 (2018).
19. K. Ohtaka, "Energy band of photons and low-energy photon diffraction," *Phys. Rev. B* **19**, 5057–5067 (1979).
20. K. Ohtaka, "Scattering theory of low-energy photon diffraction," *J. Phys. C* **13**, 667–680 (1980).
21. K. Ohtaka, Y. Suda, S. Nagano, T. Ueta, A. Imada, T. Koda, J. S. Bae, K. Mizuno, S. Yano, and Y. Segawa, "Photonic band effects in a

- two-dimensional array of dielectric spheres in the millimeter-wave region," *Phys. Rev. B* **61**, 5267–5279 (2000).
22. T. Inui, Y. Tanabe, and Y. Onodera, *Group Theory and Its Applications in Physics*, Vol. 78 of Springer Series in Solid-State Sciences (Springer, 1996).
 23. K. Sakoda, "Proof of the universality of mode symmetries in creating photonic Dirac cones," *Opt. Express* **20**, 25181–25194 (2012).
 24. B. Zhen, C. W. Hsu, Y. Igarashi, L. Lu, I. Kaminer, A. Pick, S.-L. Chua, J. D. Joannopoulos, and M. Soljačić, "Spawning rings of exceptional points out of Dirac cones," *Nature* **525**, 354–358 (2015).
 25. Y. Liang, C. Peng, K. Ishizaki, S. Iwahashi, K. Sakai, Y. Tanaka, K. Kitamura, and S. Noda, "Three-dimensional coupled-wave analysis for triangular-lattice photonic-crystal surface-emitting lasers with transverse-electric polarization," *Opt. Express* **21**, 565–580 (2013).
 26. W. Suh, Z. Wang, and S. Fan, "Temporal coupled-mode theory and the presence of non-orthogonal modes in lossless multimode cavities," *IEEE J. Quantum Electron.* **40**, 1511–1518 (2004).
 27. A. Volya and V. Zelevinsky, "Non-Hermitian effective Hamiltonian and continuum shell model," *Phys. Rev. C* **67**, 054322 (2003).
 28. M. Heuck, P. T. Kristensen, Y. Elesin, and J. Mørk, "Improved switching using Fano resonances in photonic crystal structures," *Opt. Lett.* **38**, 2466–2468 (2013).
 29. M. F. Limonov, M. V. Rybin, A. N. Poddubny, and Y. S. Kivshar, "Fano resonances in photonics," *Nat. Photonics* **11**, 543–554 (2017).
 30. Y. Zhang, W. Liu, Z. Li, Z. Li, H. Cheng, S. Chen, and J. Tian, "High-quality-factor multiple Fano resonances for refractive index sensing," *Opt. Lett.* **43**, 1842–1845 (2018).
 31. J. Jin, X. Yin, L. Ni, M. Soljačić, B. Zhen, and C. Peng, "Topologically enabled ultra-high-Q guided resonances robust to out-of-plane scattering," arXiv:1812.00892 (2018).
 32. A. Krasnok, R. Savelev, D. Baranov, and P. Belov, "All-dielectric nanophotonics: fundamentals, fabrication, and applications," in *World Scientific Handbook of Metamaterials and Plasmonics* (World Scientific, 2017), pp. 337–385.
 33. Z. Sadrieva, K. Frizyuk, M. Petrov, Y. Kivshar, and A. Bogdanov, "Multipolar origin of bound states in the continuum," arXiv:1903.00309 (2019).